Hindawi
International Transactions on Electrical Energy Systems
Volume 2023, Article ID 9403058, 21 pages
https://doi.org/10.1155/2023/9403058

Research Article

Short-Circuit Protection Schemes for LVDC Microgrids Based on the Combination of Hybrid Circuit Breakers and Mechanical Breakers

Riccardo Lazzari [1] **and Luigi Piegari** [2]

[1]*Materials and Generation Technologies Department, RSE SpA, Via Raffaele Rubattino 54, Milan 20134, Italy*
[2]*Dipartimento di Elettronica, Informazione e Bioingegneria, Politecnico di Milano, Via Ponzio 34/5, Milan 20133, Italy*

Correspondence should be addressed to Luigi Piegari; luigi.piegari@polimi.it

Received 16 November 2021; Revised 19 May 2023; Accepted 25 May 2023; Published 14 June 2023

Academic Editor: Kamran Iqbal

In recent years, low-voltage direct current (LVDC) microgrids are becoming more attractive because they represent a solution to integrate renewable sources, storage, and electronic loads bringing some advantages in comparison with traditional AC grids. However, the protection of such a network involves many challenges, especially in the case of LVDC microgrids with more than one feeder and multiple energy sources. Indeed, the traditional protection breakers used for an AC grid cannot isolate the faults and protect the components of a DC grid, while the use of solid-state circuit breakers increases energy losses. This paper deals with the analysis and design of the protection schemes for LVDC microgrids through the combination of mechanical circuit breakers and hybrid circuit breakers. This solution has the advantage of energy loss reduction but introduces further issues due to the slow transition times of the mechanical circuit breakers. Thus, a completely decentralized control system capable of overcoming the fast fault-clearing time, cost-effectiveness, and selectivity issues is designed to protect from pole-to-pole faults. The proposed control strategy is compared with a centralized protection scheme available in the literature through numerical simulation. The two algorithms show similar performances, with a mean voltage dip duration of less than 30 ms and a maximum voltage dip duration of about 100 ms in the most severe fault condition, but the proposed solution is more reliable and flexible since it does not depend on the communication system.

1. Introduction

Nowadays, the development of power electronics technology, the wider diffusion of renewable energy sources (RESs), and the integration of energy storage systems (ESSs) are supporting the realization of direct-current (DC) grids [1, 2]. The advantages of a dc grid compared to the traditional one are well known [3] and include higher energy efficiency [4] and natural interfaces with RESs, electronic loads, and ESSs [5]. In addition, dc grids do not exhibit the typical issues of AC grids, such as synchronization, frequency regulation, reactive power flow, and three-phase imbalances.

These advantages combined with the use of controllable power electronic converters will provide many benefits for the low-carbon energy transition [6]. In this context, DC transmission will play an important and increasing role in the grid for long-distance bulk power transmission with the aim of interconnecting separate power systems within a country or connecting the national grids of separate countries. Moreover, HVDC can be used for the connection of offshore wind farms [7] and to increase grid flexibility. HVDC grids can be realized with a multiterminal or a point-to-point structure that typically carries power between two different AC areas. Although HVDC is an efficient technology, some challenges need to be addressed for its wide diffusion, such as the availability of fast and lossless circuit breakers, the detection, location, and clearance of faults, and the availability of HVDC grid codes to achieve technical standardization [8].

Over the past few years, low-voltage direct current (LVDC) has gained great attention from the global research community as it gives an extensive usage of renewable energy resources [1, 9]. Compared to an HVDC network, an LVDC grid works with a low voltage (<1500 Vdc), and thus, it is less complex from the converter's and circuit breakers' points of view, but it suffers from a lack of standardization of voltage levels and power quality that is still the main challenge to the widespread adoption of this technology. Moreover, an LVDC grid has more nodes and components than an HVDC grid, such as distributed generators, loads, and energy storage systems which makes the adoption of this technology more challenging. Indeed, an LVDC microgrid introduces several converters with various characteristics into a system with low inertia and without a natural zero-crossing current with possible stability and protection problems [10].

In such a system dominated by power electronics, the design and control of these converters are of great importance. However, converter control schemes are generally designed to achieve voltage regulation and current (or power) sharing [11], but in control design, the power converters dynamics are often omitted or described by linear models [12]. However, power electronic converters have limitations due to their characteristics and topology which can add further instability to the system. The interface of a load through a converter introduces a constant power load (CPL) that is nonlinear and time-dependent and has a negative incremental impedance which can deteriorate the system stability. Various stabilization techniques have been proposed in the literature [13, 14] which are mainly based on ideal CPLs to include their nature of negative incremental impedance. However, the assumption of an ideal CPL does not regard the influence of the controller design and operating conditions on the system stability. The characteristic impedance of the converter, its output power, and its control bandwidth indeed influence the stability margin [15] and must be taken into consideration in the development of the control structure of the LVDC microgrid. However, DC microgrids are a complex system due to a high number of energy sources, with uncertainty in power generation, nonlinearities introduced by power converters, and the interaction between the dynamics of converters operating with different modes [14].

Protection is another crucial topic for the future development of LVDC microgrids. Indeed, this type of grid introduces a complex mix of power converters with different typologies, which require filter capacitors to mitigate the voltage ripples. In the case of a dc bus short circuit, these capacitors rapidly discharge into the fault, causing a current surge with an amplitude that depends on the filter design and location of the fault [16]. It is worth noting that not all converters can block the fault current. Indeed, when the capacitor voltage drops, the antiparallel diodes of voltage source converters (VSCs) and boost converters will be forward-biased, and the source will continue to supply the fault [17] even if the converter is turned off. Because the diodes can only withstand a certain level of current, the fault must be detected and eliminated very quickly to protect the converters.

To prevent damage and promptly isolate a fault from the grid, Bui et al. proposed the use of fast-acting fuses, which can protect a dc microgrid with a short critical fault-clearing time and limited cost [18]. Nevertheless, this protection cannot be automatically restored after the fault, causing an outage in the faulty part of the grid. To solve this issue, Peng and Huang suggested the use of a semiconductor switch in series with the capacitor of the dc link [19]. This solution limits the fast rising of the discharge current of the capacitors but affects the voltage of the dc grid and cannot prevent the conduction of the antiparallel diodes of the converters. Baran and Mahajan proposed a hardware modification of the power electronic converters through the replacement of the freewheeling diodes of the VSC with other IGBTs and the design of smoothing capacitor branches [20]. This solution makes it possible to quickly limit the fault current, but new challenges arise in the development of a protection scheme that can detect and locate faults.

The protection of a dc microgrid faces many challenges involving fault detection and location, equipment durability, and fault ride-through capability [21]. Patil and Satarkar suggested the use of a ring-type LVDC distribution system protected by solid-state circuit breakers (SSCBs) installed at the terminal point of each line [22]. This solution guarantees a high breaking speed and the ability to withstand high short-circuit currents, but the use of IGBT causes an increase in energy losses [23]. To protect a multiterminal dc grid with limited losses, Hernández et al. suggested a combination of SSCBs and hybrid circuit breakers (HCBs) [24]. Although this combination of HCBs and SSCBs reduces the energy losses, the installation cost increases.

For this reason, this paper proposes a combination of HCBs and mechanical circuit breakers (MCBs) to reduce both the cost and energy losses. This paper deals with the integration of the traditional MCBs and the HCB proposed in [25]. This novel hybrid circuit breaker can trip the circuit during normal operation and fault conditions, preventing overcurrent and overvoltage on the breaker and dc grid's components. The proposed structure can also open during a short circuit using its internal inductances to partially limit the increase in current.

The use of MCBs reduces costs but introduces further issues. Indeed, MCBs have slow transition times because of the need to blow the arc in the extinguishing chamber, and the lifetime is reduced in the case of high-current interruptions. For this reason, the HCBs and MCBs in a dc microgrid must be coordinated to protect the system and reduce the maintenance of the mechanical breaker. In this situation, it is essential to develop a well-designed protection scheme. Lazzari and Piegari proposed a centralized controller to coordinate the intervention of the converters and the HCBs installed in the grid for ensuring protection from a pole-to-pole short circuit in a low-voltage dc grid [26]. This control strategy allows fast fault-clearing time and selectivity, but due to its centralized structure, it must be updated at any new installation of RESs or any time the grid topology changes. Moreover, in case of faults in the communication

line, the selectivity of the intervention is not ensured, and the whole grid could remain out of service until a human intervention restores the correct operation.

This paper deals with the analysis of a completely decentralized protection scheme for a low-voltage dc microgrid with several renewable generators, energy storage systems, loads, and VSCs that interface with the AC grid. Firstly, the paper analyses the protection issues of LVDC grids by evaluating the system behaviour during a pole-to-pole fault using numerical simulations. Starting from the results of this analysis performed through an LVDC benchmark, the protection devices' positioning is evaluated by considering the installation of both MCBs and HCBs. Finally, a completely decentralized control strategy is proposed, and it is compared with the one of [26] using numerical simulations of pole-to-pole faults on dc test microgrids. From the comparison, it is shown that the performances of the proposed decentralized controller are comparable with the performances of the centralized one. Nevertheless, it does not rely on a communication line, and it does not need to be updated when the grid topology changes. Finally, the decentralized control strategy proposed in this paper could be used as the first choice or as a backup control strategy in case of failure of the communication line.

The paper is organized as follows. Section 2 illustrates the impact and the issues of a pole-to-pole and pole-to-ground fault on a DC system and presents a literature review about protection schemes and breakers for LVDC grids. Section 3 addresses the effect of a short-circuit incident in an LVDC microgrid to individuate the placement of the HCBs and MCBs. In Section 4, the centralized protection scheme of [26] is recalled, the new decentralized controller is proposed, and finally, these two schemes are verified and then compared resorting to simulations. Finally, some conclusions are given in Section 5.

2. DC Fault Types and Protection Methods

A fault in a DC system can be classified as (a) a positive to negative pole short circuit (pole-to-pole fault) and (b) a positive or negative pole-to-ground fault. A pole-to-pole fault occurs when a path between the positive and negative poles is created, and it can be due to a short circuit or an internal converter fault. The latter is a terminal fault that cannot be cleared by DC grid protections. However, when a short circuit between two lines occurs, the fault must be detected and eliminated very quickly to avoid any damage to VSCs and boost converters. In this situation, as shown in Figure 1(a), the DC-linked capacitors C_{out} will discharge through the fault with current i_{fault} limited only by the line inductance L and resistance R as expressed in

$$i_{fault}(t) = \frac{V_{dc}(0)}{L\omega_d} e^{-\alpha t} \sin(\omega_d t) + i_{dc}(0) e^{-\alpha t} \left[\cos(\omega_d t) - \frac{\alpha}{\omega_d} \sin(\omega_d t) \right], \tag{1}$$

where $\omega_d = \sqrt{\omega_0^2 - \alpha^2}$, $\omega_0 = (1/\sqrt{LC_{out}})$, $\alpha = (R/2L)$

This causes the system voltage to collapse with a consequent impossibility to block the fault current provided by these converters (Figure 1(b)). Indeed, after the capacitor discharge stage, the electronic switch $S_1 \ldots S_n$ cannot be controlled, the antiparallel diodes of VSCs and boost converters $D_1 \ldots D_n$ will be forward-biased, and the converters act uncontrollably. The current in the fault during this phase is expressed in (2), and the current flow through the antiparallel diodes:

$$i_{fault}(t) = I_0 e^{-(/)t}, \tag{2}$$

where $I_0 = i_{fault}(t_1)$, where t_1 is the time when the capacitor voltage drops down to zero.

The source V_s is then directly connected to the DC grid by means of the input inductors L_{in} and continues to supply the fault [17] even if the converter components are turned off (Figure 1(c)). In the case of a VSC, the current is expressed in

$$i_{fault}(t) = i_{D1} + i_{D3} + i_{D5} = i_{ga,(>0)} + i_{gb,(>0)} + i_{gc,(>0)}, \tag{3}$$

where $i_{ga,(>0)}$, $i_{gb,(>0)}$, $i_{gc,(>0)}$ are the positive values of each phase current. For $i_{ga,(>0)}$, this current is equal to

$$i_{ga}(t) = I_g \sin(\omega_s t + \alpha - \phi) + I_{gn} e^{-t/\tau}, \tag{4}$$

where ω_s is the grid angular frequency, $\phi = \arctan[\omega_s (L_{in} + L)/R]$, $\tau = (L_{in} + L/R)$, $I_{gn} = [I_{g0} \sin(\alpha - \phi_0) - I_g \sin(\alpha - \phi)]$, and I_{g0}, ϕ_0 denotes the initial grid amplitude and phase. In the case of a boost converter, the current is expressed in

$$i_{fault}(t) = \frac{V_s}{R} e^{-(/)}, \tag{5}$$

where $\tau = (L_{in} + L/R)$. For both VSC and boost converter, the magnitude of the steady-state fault current is lower than the transient current, but it remains for a longer period if not interrupted [27]. Therefore, the diodes will be damaged without an appropriate protection scheme.

The behaviour of the system during pole-to-ground fault is strongly influenced by the grounding configuration of the LVDC and the connected AC grid. In general, the DC grounding options can be classified into three types: unearthed DC system, earthed DC system, and solidly earthed DC system. Compared with other grounding methods, the unearthed DC system has a lower ground leakage current, simpler implementation, and lower installation cost. Moreover, an unearthed DC system provides better reliability of power supply as the system operation is not influenced by a single pole-to-ground fault. However, in the case of a hybrid AC-DC network, in which the neutral point of the AC grid is grounded on the MV/LV transformer, the occurrence of a pole-to-ground fault on the DC side causes a zero-sequence current flowing through the AC/DC converter [28]. In the case of an earthed DC system, one pole or the neutral point of the system is earthed via a low or a high impedance. A single pole-to-ground fault determines the circulation of a fault current limited by the ground impedance. In this case, the main issue is related to fault

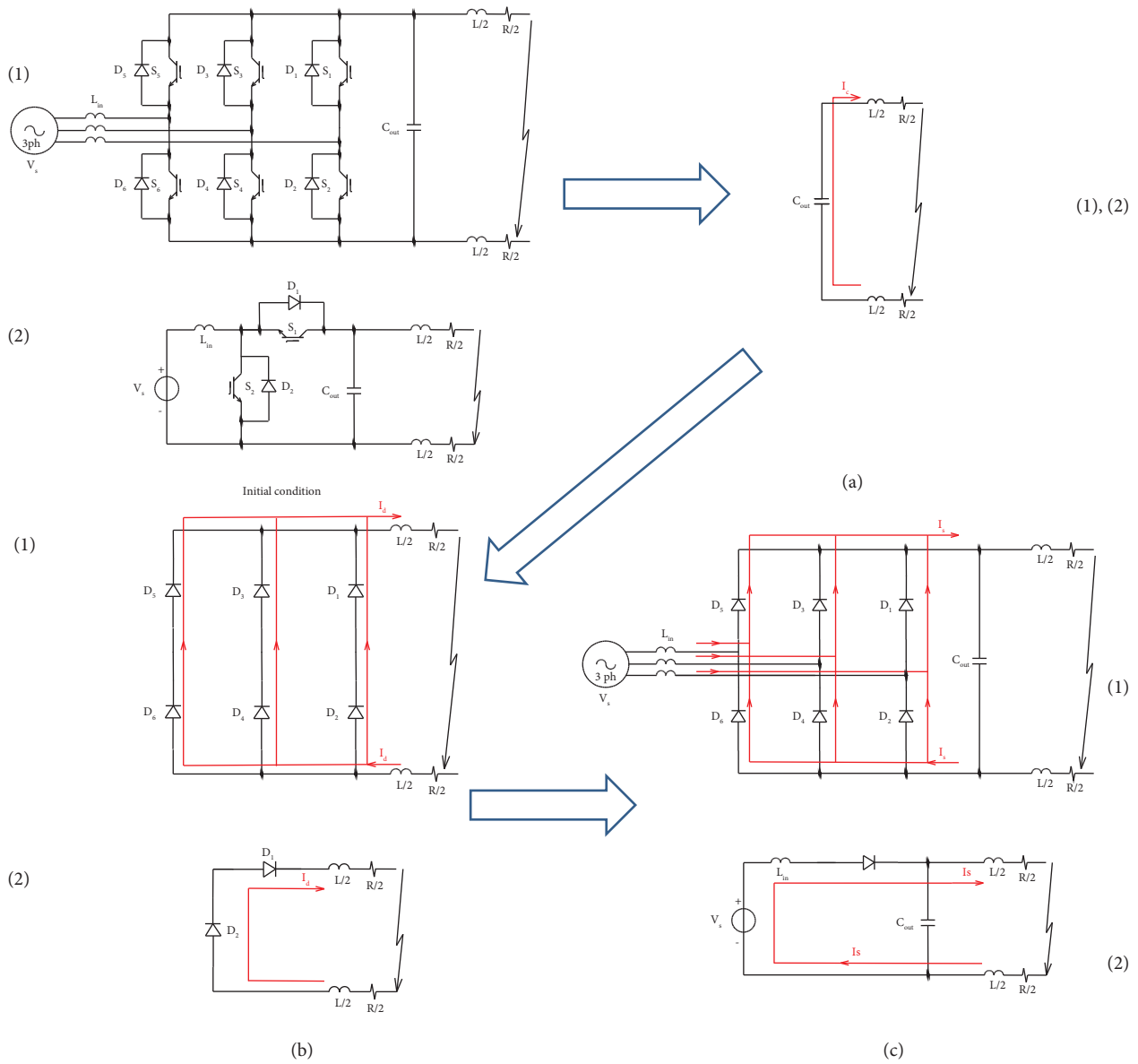

Figure 1: Transient stage during pole-to-pole fault: (1) VSC and (2) boost converter. (a) Capacitor discharging stage, (b) free-wheeling stage, and (c) current feeding stage.

measurement and detection because the faulty current becomes small. Finally, in the case of a solid earthed DC system, one pole or the neutral point of the system is connected to the earth without any impedance between them. In this situation, a single pole-to-ground fault determines a short circuit between the two poles or between a pole and the neutral point of the system, with the same issue explained for a pole-to-pole fault.

In general, the impedance of pole-to-pole fault is low, while the impedance of pole-to-ground fault can be either low or high [29]. For the analysis proposed in this paper, the pole-to-ground fault was not considered because although pole-to-pole faults are less probable than pole-to-ground faults, this type of fault causes the most serious condition for the converters [30].

2.1. Protection Devices for DC Microgrid. To prevent damage and promptly isolate a pole-to-pole fault, different breaker topologies can be used. A DC circuit breaker must ensure the following requirements: (i) low power losses, (ii) fast interruption without stress during breaking, and (iii) high dielectric strength to isolate the two sides of the breaker after the interruption [31]. Mechanical circuit breakers (MCBs) are widely used as protection devices in both AC and DC grids and comply with the first and third requirements. However, the absence of natural zero-crossing makes arc extinction difficult. Thus, an MCB cannot offer a quick and reliable operation [32].

On the other hand, solid-state circuit breakers (SSCBs) offer a high breaking speed and the ability to withstand high short-circuit currents [23]. Appropriate power

semiconductors are used to operate as a circuit breaker offering the advantage of a very short interrupting time and the absence of phenomena such as arc, contact erosion, and bounce. However, the use of IGBT causes higher energy losses than an MCB. Furthermore, to allow bidirectional operation, two unidirectional SSCBs must be connected in "antiseries" causing double the resistance in the on-state of a unidirectional SSCB, with consequent nonnegligible power losses for an LVDC system [33]. Thus, the application of the SSCBs is strictly limited to applications where fast off-transition is the essential requirement, and the losses are manageable.

For this reason, recently, considerable progress has been achieved in combining MCBs and semiconductor devices to realize HCBs [32]. In an HCB, during normal operation, the current flows through the MCB which offers a very low resistance path. When the fault is identified, the current is commutated from the MCB to the parallel solid-state path that realizes a fast and arc-less transition from the conduction to the blocking state. In this way, the solid-state part is crossed by current only during the interruption stage, avoiding the use of a bulky cooling system. Nevertheless, the cost of these breakers is higher than an MCB, and thus, it is necessary to resort to a limited number of these devices.

2.2. DC Microgrid Protection. The main purpose of a protection scheme is first to detect and identify the faulty section in the shortest possible time. Then, once the fault is recognized, the faulty section must be isolated to prevent damage to power electronic devices. Up to now, several methods have been proposed to detect and identify the faulty, and the most applied methods include overcurrent, directional overcurrent, derivative, distance, and differential protections [23]. Each protection method has different features in terms of speed, selectivity, sensitivity, reliability, and cost.

2.2.1. Overcurrent Protection. Like the traditional AC overcurrent protection, a fault is detected and isolated when the current reaches values above the overcurrent threshold. To properly isolate the fault, overcurrent relays must be coordinated. However, in the DC microgrid, due to the low value of line resistance and the high value of fault rising rate in the DC microgrids, the relay coordination based on time-current curves is a challenge. It may result in either long fault clearance times or the disconnection of larger parts of a DC microgrid. Therefore, to improve the selectivity, overcurrent protections are proposed in combination with under-voltage measurement [20]. Another solution to rise selectivity performance is to use a communication link between the overcurrent relays, but in this case, the infrastructure cost is highest.

2.2.2. Directional Overcurrent Protection. Directional overcurrent protection improves the selectivity of an overcurrent protection introducing the measurement of the current direction. After a rapid variation in the current and voltage magnitude, the current direction is sensed and used for establishing fault location through a master intelligent electronic device (IED) [34]. The directional overcurrent protection is suitable for a DC microgrid with a communication system. Thus, like all communication-based protection schemes, it suffers from communication delays and failures. Additional infrastructural costs due to communication channels and computational units are further demerits of this protection scheme.

2.2.3. Derivative Fault Protection. Current derivative protections aim at interrupting fault before the DC grid capacitor currents attain the peak. This protection method utilizes the measurement of current and/or voltage profile derivatives to estimate the equivalent inductance between the device and the fault location, determining whether the protection device should react. This kind of protection is governed by a central processing unit that detects and locates the fault based on the current derivative values of each protection device. The highest among the current derivative values for each protection device detects the fault [35]. In real practice, this method needs high bandwidth communication link, and fast and accurate data synchronization and is affected by the measurement noise introduced from the current/voltage sensing devices, which undermines the overall protection performances [36].

2.2.4. Differential Protection. Differential protections offer a suitable protection method for both AC as well DC microgrids as the detection accuracy, and sensitivity is not affected by the load, distributed generation (DG), and short-circuit fault magnitudes [37]. Typical differential protection protects the system by using and comparing the current measurements at each side of a specific line or feeder. Through the communication between two relays, located at the ends of the line, this protection scheme calculates the current difference between the two ends of the line and activates the trip signal if this differential current exceeds a threshold. Differential protection is a fast and accurate method to detect a fault in a DC microgrid, but it requires good synchronization between the two relays to avoid trips even in normal operating conditions [38]. Yet, due to fast and accurate communication means, this protection method is expensive.

2.2.5. Distance Protection. Also known as the impedance estimation method, its working principle is based on the estimation of the fault loop impedance through the synchronous measurement of current and voltage [39]. This quantity is then used to evaluate the distance between the point of measurement and the fault location. If this measurement is within a given distance value, a tripping signal will be sent to the associated circuit breaker after a specific time delay. This method is a common and effective protection for AC systems, but in DC, systems small impedance and the absence of a fundamental frequency are the main obstacles to adopting this method. The active impedance

estimation (AIE) technique [40] improves the fault localization thanks to the injection of a triangle current waveform once the faulty condition is recognized. However, this method requires additional equipment to inject transient current and record the bus transient voltage to evaluate the line impedance. This increases the cost of the protection system due to the deployment of current injection units, high bandwidth measurement, and computational units.

2.3. Proposed Method. As explained in the previous section, an LVDC microgrid can be protected using breakers suitably managed by different protection schemes. However, protecting a DC microgrid in case of pole-to-pole fault is challenging due to the possible damage to the power converters. The use of SSCBs in combination with communication-based protection schemes allows to detect DC faults very fast and accurately, but due to the communication requirements, this protection scheme is expensive [36]. Moreover, resorting to only SSCBs reduces the energy efficiency of a DC grid. The additional infrastructural cost due to communication channels and computational units are further demerits that should be considered during the design of a protection scheme.

2.3.1. Main Objective. The scope of this work is to develop a protection scheme that can offer low costs and high energy efficiencies. This is achieved by minimizing the number of hybrid circuit breakers and by combining HCBs and MCBs with a communication-less protection scheme. Although the absence of a communication system reduces the speed of fault detection, this solution is not affected by the failure, delay, and synchronization problems that make it difficult to ensure system protection. Moreover, in the design of the protection architecture, the installation of the HCBs is performed considering the current circulating during a fault. In particular, the HCBs are installed only to protect the nonlimited converters that must be disconnected as soon as a fault is recognized. This is done through the HCB proposed in [25] and shown in Figure 2 which can trip the circuit during normal operation and a fault condition, preventing overcurrent and overvoltage on the breaker and DC grid's components. This breaker can also open during a short circuit using its internal inductances to partially limit the increase in current, providing high efficiency and a long lifetime. During normal operation, this breaker offers a low resistive path composed by the mechanical breaker T and the inductors L and L_{out}, while the capacitor C is maintained charged through the electronic switch S_2. To trip the breaker, S_2 is turned off while S_1 is turned on connecting the capacitor C in parallel to T. In this way, the current flowing in T is inverted and maintained in a range near zero acting on S_1 by means of a hysteresis control. Thus, the mechanical breaker can be opened with a current near zero and a limited arc. It is worth noting that the output inductance L_{out} is used to limit the overvoltage on the load when the breaker opens, and it allows a current limitation during a short circuit for the time necessary to open the circuit.

In this way, once the nonlimited converters are protected, the current circulating in the fault is limited, and all other feeders can be protected with a breaker capable of opening only the maximum current of the line. In this way, as soon as the current in the faulty line drops below the maximum manageable current, its breaker can open. This allows MCBs to be used without oversizing.

2.3.2. Protection Scheme. As explained previously, the protection scheme is designed to manage a pole-to-pole fault resorting to a reduced number of HCBs and MCBs. When a fault appears, the current in the pole-to-pole fault is provided by each limited and nonlimited source:

$$I_{fault}(t) = \sum_{k}^{\aleph_{NL}} i_{NL,k}(t) + \sum_{k}^{\aleph_{L}} i_{L,k}(t), \tag{6}$$

where $i_{NL,k}$ is the current provided by the k-th nonlimited source, and $i_{L,k}$ is the one provided by the k-th limited source.

Resorting to HCBs to each nonlimited converter allows disconnecting these devices before reaching the freewheeling stage (Figure 1(b)) and limiting the faulty current to the sum of the maximum currents $i_{L_{\text{Max}},k}$ that can be provided by limited sources:

$$i_{fault} = \sum_{k}^{\aleph_{L}} i_{L_{\text{Max}},k}(t). \tag{7}$$

In this situation, even if the faulty current is limited, the breaker of the faulty feeder must be designed to interrupt a high current in the case of a high number of limited sources. This can make it necessary to also use HCBs for the feeders because these can open a short-circuit current, which increases the installation cost of the DC microgrid. However, to solve this problem, it is possible to define a protection scheme capable of reducing the current in the faulty feeder to a lower value before the breaker trips. To make this strategy effective it is necessary to disconnect the limited sources in case of fault and, therefore, limited sources must be capable of identifying the faulty condition autonomously. Limited sources cannot detect a failure with a simple current threshold. Using a current threshold, the sources would disconnect each time they reached saturation even in the event of a simple temporary overload. For this reason, the opening of the limited sources derives from the occurrence of two conditions: the achievement of a current close to the maximum and a terminal voltage under a certain threshold. This last threshold depends on the components of the DC grid and must be defined considering the grid structure. The overall voltage of the DC grid, after the disconnection of the nonlimited source, is in fact sustained only by the limited source and reaches the value expressed in (7):

$$V_{dc} = R_{fault} \sum_{k}^{\aleph_{L}} i_{L_{\text{Max}},k}. \tag{8}$$

Once the limited sources are disconnected, the current in the faulty line drops below the maximum manageable

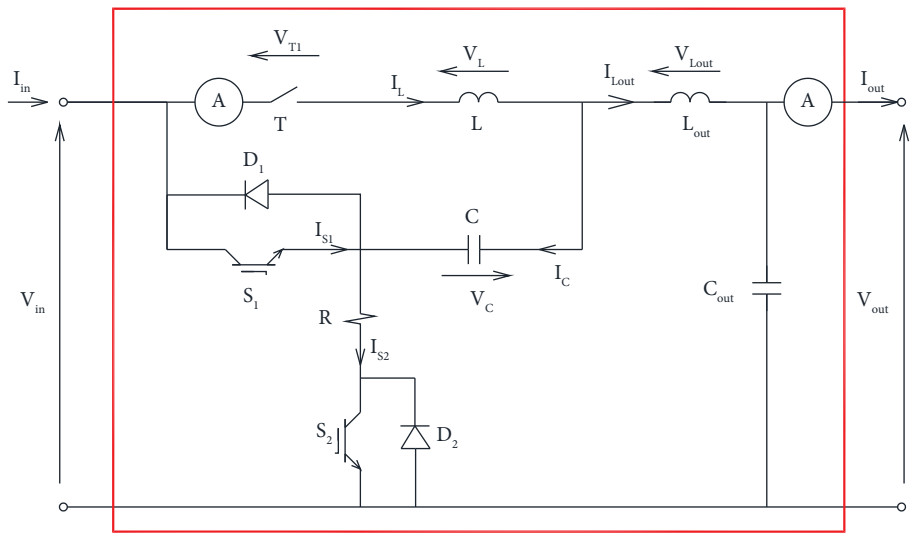

Figure 2: Hybrid circuit breaker [25] used in this study.

current and the breaker can open. Once the faulty line is opened, the sources can be reconnected, and the DC grid can be restored after a transitory disconnection. However, it shows very interesting performances as indicated in Table 1 and allows the use of traditional MCBs and HCBs reducing the overall cost of the infrastructure and increasing the efficiency of the DC grid.

3. Short-Circuit Occurrence in an LVDC Microgrid

This section illustrates the effect of a pole-to-pole fault on an LVDC microgrid. The analyses were carried out on an LVDC benchmark by means of a simulation model realized in Matlab/Simulink through the toolbox Simscape Electrical™. Finally, the protection device's location is presented and verified.

3.1. DC Microgrid Benchmark. To analyse the possible protection schemes, a DC microgrid benchmark was built based on the AC microgrid benchmark proposed in [41], which was opportunely modified to consider a voltage level of 380 V and a unipolar distribution. The rated power of the grid is 75 kW, and a two-bidirectional AC/DC converter supplies the grid. The benchmark was defined considering various components, such as PV fields, wind generators, several loads with different characteristics, energy storage systems, and two front-end converters with the AC main grid. Furthermore, different converters typologies were considered to verify the necessary protection devices. These components are listed in Table 2, while the schematic of the LVDC microgrid benchmark is shown in Figure 3. The sections of the lines were calculated to maintain a voltage drop lower than ±5% and considering PCU/XLPE/PVC 600/1000 V cables. The parameters of the lines are indicated in Table 3. For the simulations, all the converters have been modelled using the well-assessed switching model in which the switching transients are neglected. Switching losses do not affect the behaviour of the system in the simulated scenario. For what concerns the HCB, the model proposed in [25] has been used. Batteries have been simulated as an ideal voltage source while for the PV systems, the well-known single-diode model [42] was adopted. It is worth noting that the models used for the sources do not strongly affect the behaviour of the system in the fast transients of the simulated short-circuit scenario during which the capacitors have a dominant effect. Nevertheless, using an ideal voltage source for the battery represents a conservative solution for the short-circuit analysis.

3.2. Short-Circuit Simulation Results. To verify the behaviour of the DC microgrid in the case of a short circuit, simulations were carried out through Matlab/Simulink®. The model of the DC microgrid has been realized by resorting to the Simscape Electrical™ toolbox, and every simulation, shown in the rest of the paper, is performed resorting to the variable-step solver Ode23t. The simulations discussed in this section were performed without protection devices and considering that load 1 and load 2 had resistances of 10 Ω, and photovoltaic 2 was working at its maximum power of 3.3 kW. During the simulation, four different converters were considered. The parameters of the different converters are indicated in Table 4. No other converters for the grid were used during the simulations. Simulations were carried out resorting to simple battery and photovoltaic models because they had no impact on the simulation results.

Starting from a steady-state condition, at time $t = 0.2$ s, a short circuit with a resistance of 10 mΩ occurred at the feeder of load 2. During the fault, the voltage of each node dropped, as shown in Figure 4. These voltage drops were different in each node based on the fault's location and the source's typology. Indeed, despite Battery 1 being closer to the fault than Inverter 1, the voltage was higher for Battery 1's node. As shown in Figure 5, the current provided by Battery 1 was greater than the current of Inverter 1.

Table 1: Comparison between different protection schemes.

Method	Speed	Selectivity	Sensitivity	Reliability	Cost	Advantages	Disadvantages
Overcurrent protection	Medium	Low/ Medium	Low/ Medium	Medium	Low	(1) Simple method (2) No communication link that improves reliability	(1) Vulnerable to noise and other disturbances (2) Requires a communication link to increase selectivity and coordination
Directional overcurrent protection	Medium	High	Low/ Medium	Medium	Medium	(1) Applicable for networks with different types of DGs	(1) Requires a communication system to a central processing unit
Derivative fault protection	High	Low	High	Low/ Medium	High	(1) Discriminates internal and external faults	(1) The rate of change of current is highly sensitive to fault impedance, and it is difficult to design an appropriate di/dt protection scheme (2) Requires a communication system to a central processing unit (3) Needs fast and accurate data synchronization (4) Requires SSCB to achieve high-speed performances
Differential protection	High	High	High	Medium	Very high	(1) Reduced dependency on the fault impedance and rate of rise of current (2) Not dependent on the current direction	(1) Requires high bandwidth communication link between device terminals (2) Errors with communication link impacts its reliability (3) Unsatisfactory performance in noisy conditions (4) Needs fast and accurate data synchronization (5) Requires SSCB to achieve high-speed performances
Distance protection	Medium	High	Low/ Medium	Medium	Medium	(1) Identification of the fault location	(1) More sensitivity to fault resistance (2) Limited accuracy in short lines and for DC systems (3) Requires synchronization between voltage and current measurement
Proposed method	Medium	Medium/ High	Medium	High	Low	(1) Simple method (2) Applicable in DC grids with different types of DGs (3) No communication link that improves reliability (4) Can be applied in DC grid with traditional MCBs	(1) Requires the transient disconnection of the sources

Table 2: LVDC benchmark components' main characteristic.

Component	Pnom	Typology
Inverter 1	75 kW	Voltage source converter
Inverter 2	75 kW	Voltage source converter
Battery 1	45 kW–90 kWh	Boost converter
Battery 2	50 kW–50 kWh	Buck converter
PV 1	3.3 kW	Boost converter
PV 2	10 kW	Buck-boost converter
Wind Generator	10 kW	Rectifier and boost converter
Load 1	15 kW	Z constant
Load 2	15 kW–6 kW	Z constant–P constant
Load 3	12 kW	Z constant–P constant
Load 4	4.5 kW	I constant
Load 5	15 kW–7.5 kW	Z constant–I constant

Considering this scenario, during a fault in the DC microgrid, the converter of Battery 1 tries to reduce its duty cycle, but it reaches the minimum value without any possibility of limiting the current. Under this condition, if the converter is turned off, the antiparallel diode of the output transistor is forward-biased, and Battery 1 is directly connected to the DC grid. Inverter 1 presents an overcurrent due to the conduction of the antiparallel diodes. When the DC grid's voltage drops, these components are forward-biased, and controlling the converter is not able to limit the current. The photovoltaic converter shows an initial overcurrent due to the output capacitor discharge, but after that, the current is limited because this source has finite power. At the same time, the converter of Battery 2 can limit the current because there are no forward-biased diodes. Thus, the control can modulate the current acting on the switching characteristic of the transistors.

From this analysis, it is clear that sources with limited power, such as the PV plant, or those connected through self-limited converters, such as the one used for Battery 2, do not need fast circuit breakers capable of opening to stop a current that could be unlimited, while it is necessary to protect the other types of sources.

3.3. Protection Device Location. Considering the analysis presented in the previous section, it is worth noting that intrinsically nonlimited sources must be equipped with HCBs, like the one shown in Figure 2. In this way, the current circulating during a fault is limited, and all the other feeders can be protected with a breaker capable of opening only when the maximum current of the limited sources is reached.

These protection devices can be realized either with traditional breakers or with the hybrid circuit breaker sized to open only under a limited current. Furthermore, the protection devices for the sources must be bidirectional or unidirectional depending on the type of source. In any case, the ability to open under a short-circuit condition must be guaranteed only in one direction. In contrast, the breaker of the feeders must be able to open under short-circuit currents in both directions. This is true for all the feeders to which at least one source or storage system is connected. These protection devices can be sized to open only under the maximum current and can be realized through two unidirectional HCBs connected in antiseries. The trip time of the feeder protections must be appropriately slower than the source protection systems. This ensures that the opening occurs when the DC grid is no longer able to sustain a current higher than the nominal one. After the isolation of the faulty feeder, the sources can be reclosed on the DC grid. The positions of the different protection devices are illustrated in Figure 6.

To verify these statements, a simulation was performed considering the use of hybrid circuit breakers for Inverter 1 and Battery 1, capable of opening under a short-circuit condition, with a trip threshold of 375 A. Finally, the use of mechanical breakers was considered, with a trip delay of 50 ms, installed on the faulty feeder. During the simulation, after a delay of 100 ms, the sources connected through the HCBs were reclosed. It is worth noting that to achieve a reconnection without transients, the converter regulators needed to be reset after the breaker tripped. Thus, the controller of the converters had to be integrated with the protection. At time $t = 0.2$ s a fault occurs, after 50 ms, the faulty feeder opens, and at the time $t = 0.3$ s, the HCBs of the sources were reclosed.

Looking at the voltage graph shown in Figure 7, it is possible to observe an immediate voltage drop when the fault occurs. In the first milliseconds, this voltage drop is limited by the current provided by all the converters and remains quite contained. After a few milliseconds, the HCBs of Inverter 1 and Battery 1 open, causing a further rapid decrease in the voltage, which is sustained at over 100 V by Battery 2 and the photovoltaic panels.

Battery 2 supplies its maximum current of 250 A, as shown in Figure 8, while the photovoltaic plant, after the initial overcurrent due to the output capacitor discharge, supplies a current higher than the one delivered before the fault. Indeed, the PV plant works at its maximum power point. Thus, when the voltage drops, the current increases until it reaches the short-circuit current of the panel.

After the HCBs trip, it is possible to observe that the currents of Inverter 1 and Battery 1 are not zero. These currents are due to the output capacitor of the HCBs, which are being discharged on the fault. At time $t = 0.25$ s, the fault is cleared by the opening of the breaker on the feeder where Load 2 is connected. The DC voltage starts to increase as a result of Battery 2, which continues to supply a constant current. The photovoltaic system absorbs current for a short time to recharge the output capacitor of its converter. Finally, a new steady state condition has been reached, in which Battery 2 supplies the whole DC grid, in island operation. When, at time $t = 0.3$ s, the HCBs of the two disconnected sources are reclosed, and a new voltage transient, due to their reconnection, takes place.

It should be noted that, when the fault occurs, there is a current peak that reaches about 700 A, as shown in Figure 9. This high value is due to the sum of all the sources connected to the system that temporarily supports the fault. However, after the HCBs trip, the current naturally drops to about 300 A, which is the current supplied by the limited

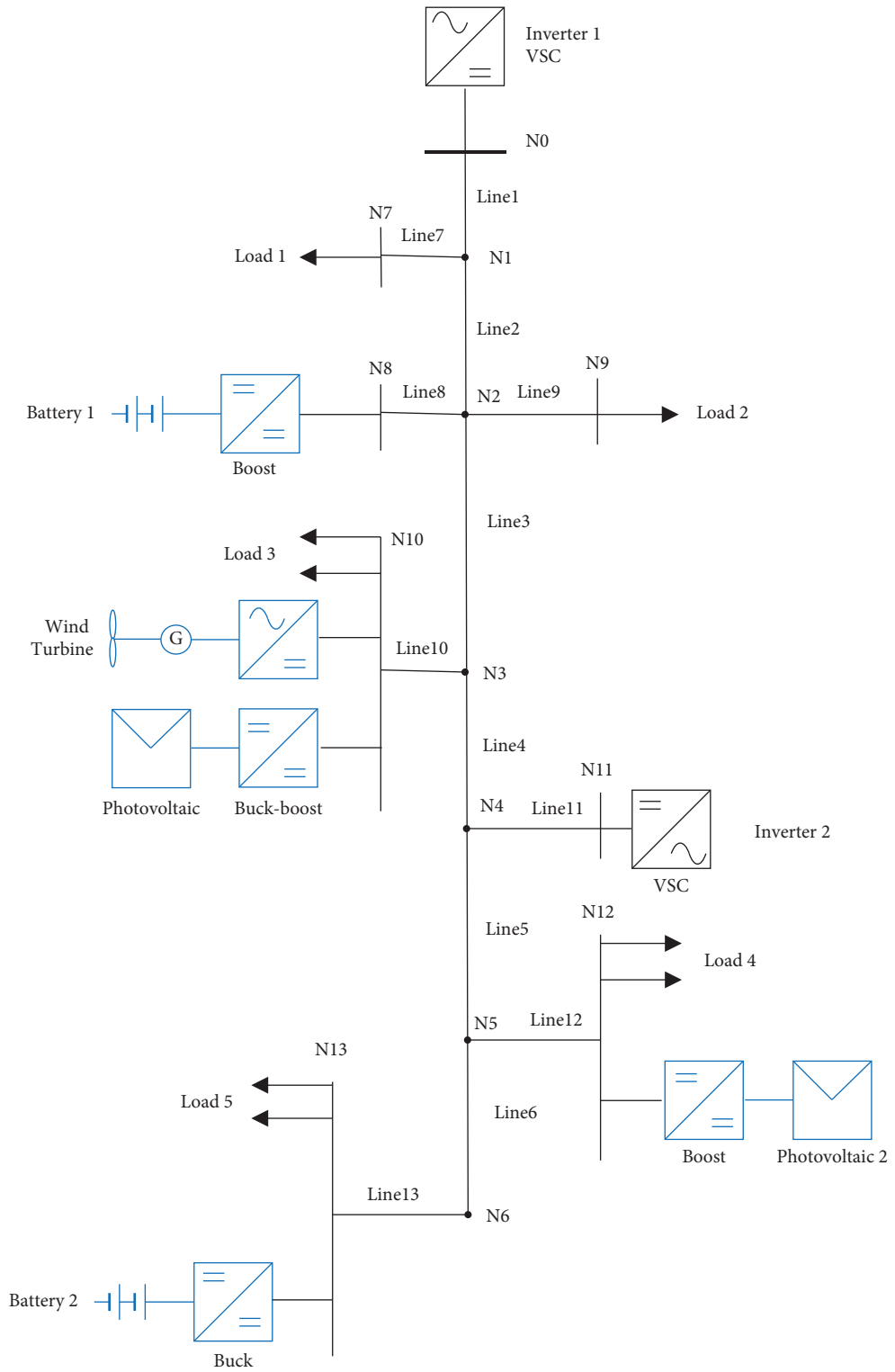

Figure 3: Schematic of the LVDC microgrid benchmark.

sources. The feeder protection must be able to open this current.

It is worth noting that if there are many limited sources in the grid, which are, therefore, not disconnected by the protections, the current that the faulty feeder breaker must interrupt can reach very high values. For this reason, it is necessary to consider this aspect when the network is sized or to define a protection scheme capable of reducing this current before the faulty feeder trips. This problem will be analysed in the

Table 3: LVDC benchmark lines' parameters.

Line segment	From	To	r (Ω/km)	x (Ω/km)	Length (m)	Section (mm^2)
Line 1	N0	N1	0.193	0.0727	35	95
Line 2	N1	N2	0.193	0.0727	35	95
Line 3	N2	N3	0.193	0.0727	70	95
Line 4	N3	N4	0.193	0.0727	50	95
Line 5	N4	N5	0.193	0.0727	50	95
Line 6	N5	N6	0.193	0.0727	35	95
Line 7	N1	N7	3.08	0.0885	30	6
Line 8	N2	N8	0.524	0.0771	30	35
Line 9	N2	N9	1.15	0.0815	135	16
Line 10	N3	10	1.15	0.0815	30	16
Line 11	N4	N11	0.193	0.0727	35	95
Line 12	N5	N12	3.08	0.0885	30	6
Line 13	N6	N13	0.727	0.0818	30	25

Table 4: LVDC benchmark converters' parameters.

Component	Inverter 1	Battery 1	Battery 2	PV 2
Typology	VSC	Boost Converter	Buck Converter	Boost Converter
Max current (A)	250	250	250	20
Input voltage (V)	400 ac 3ph	250 ÷ 330	400 ÷ 520	0 ÷ 210
Output voltage (V)	380	380	380	380
Filter inductance (mH)	0.165	1.2	1.2	1.12
DC bus capacitance (mF)	17.4	5.8	5.8	5.8

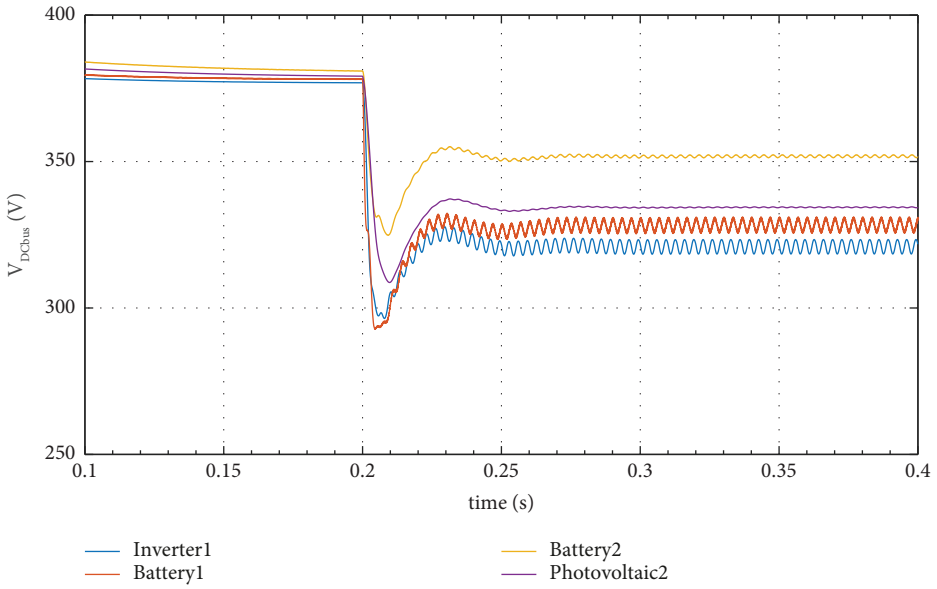

Figure 4: Voltage trend during short circuit without protection device.

following sections where two different protection schemes will be proposed.

4. Proposed Protection Scheme

This section illustrates, analyses, and compares two different schemes to protect the grid and the components in the presence of pole-to-pole faults. The former protection scheme is based on a centralized controller that receives information from all the feeder's protections while the latter is based on a decentralized structure that does not require any communication system and has the advantages of being cheaper and capable of providing a safe solution in the case of a fault in the central control unit.

4.1. Centralized Protection Scheme. This section proposes and verifies a centralized protection scheme in a simulation environment. Using a centralized controller is the easiest

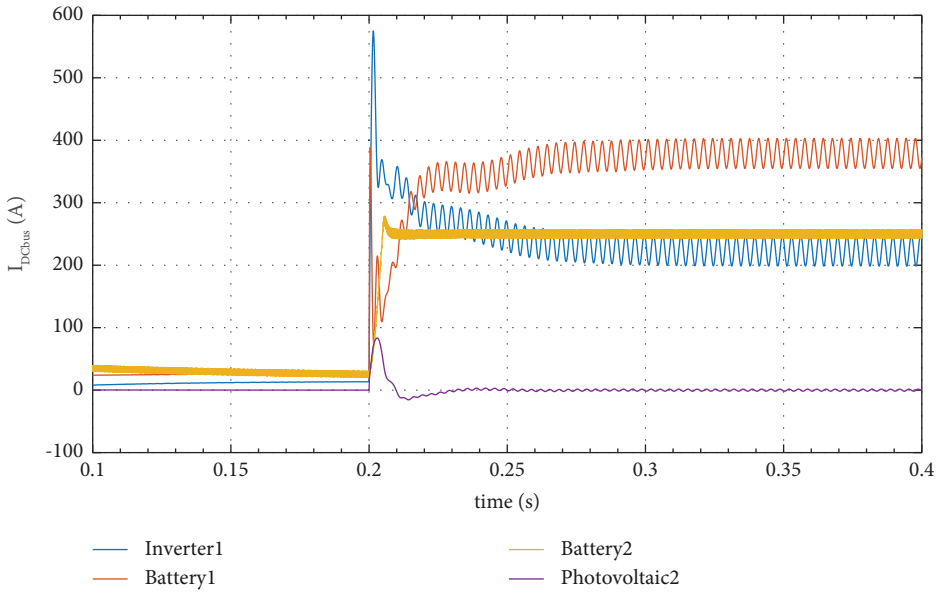

Figure 5: Current trend during short circuit without protection device.

way to guarantee the coordination of the protections. However, communication delays must be considered. For this reason and to avoid issues related to communication system errors, basic functionalities must be implemented locally. For the sake of simplicity, in this paragraph, it is assumed that there are no communication failures. In any case, it is appropriate for the HCBs of the nonlimited components to trip immediately, disconnecting the source without waiting for the centralized controller. The breaker must communicate with the controller to identify both the short-circuit current and the tripping condition. Indeed, the controller uses a series of input parameters that include the short-circuit identification, circuit breaker trip condition both for the line and for the nonlimited sources, and current values measured in the DC microgrid. The controller is realized using a state-flow approach. Based on its status, the centralized controller performs different operations as described as follows:

(i) State 0: During this state, the DC microgrid works correctly, and the controller waits for the recognition of an over-current condition. This happens if a short-circuit identification is communicated by the breakers or if the controller identifies a faulty current. If the short-circuit condition is communicated by nonlimited sources, the controller sends a current limiting signal to the limited sources and goes to state 1. If the fault is identified by the same controller, in addition to sending the limitation signal to the limited sources, the controller sends the opening command to the nonlimited sources before the transition to state 1. If the fault occurs far from the nonlimited sources, the controller must command the opening of HCBs before the current of those sources reaches the automatic trip threshold.

(ii) State 1: The controller, starting from the short-circuit signals, identifies the faulty feeder. Based on the current that the faulty line breaker can open, it may decide to keep one or more intrinsically limited sources active, completely or partially. This functionality is to be considered useful only in a case where a residual voltage for the direct current microgrid may be necessary for emergency operations. In this paper, it can be assumed that during the opening operation, the network can be completely disconnected, so that after identifying the fault location, the controller communicates to all the sources to disconnect (or in any case to bring its references to a minimum) and then waits. The controller exits this state and enters state 2 when it has received from the nonlimited sources the trip condition and the limited ones the achievement of the reference current.

(iii) State 2: As soon as the controller enters this state, it sends the trip signal to the breaker of the faulty feeder and keeps waiting until this breaker confirms the opening of the faulty feeder. When this signal is received, before returning to state 0, the controller sends a reset signal to reconnect all the sources. If automatic reclosures are integrated into the scheme, the controller resets the fault indication and sends a closing command to the breaker of the faulty feeder. After a defined number of reclosures, the controller definitively disconnects the faulty feeder and reports the need for maintenance.

The logic of the centralized protection scheme is summarized in the state-flow diagram shown in Figure 10.

To verify the effectiveness of the proposed centralized controller scheme, some simulations in Matlab/Simulink were performed. During these simulations, a cycle time for

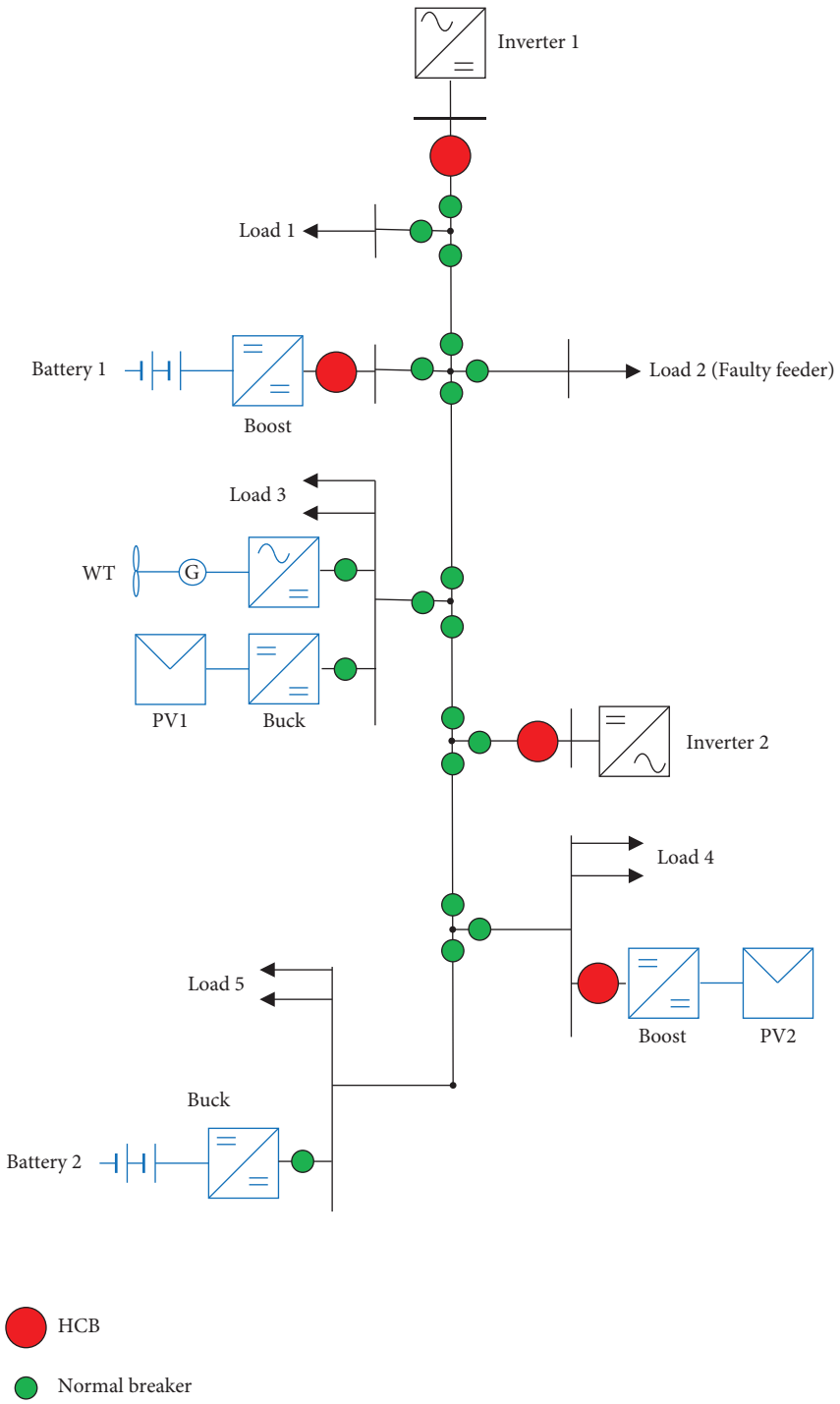

Figure 6: Breaker positions in the grid.

the controller of about 100 μs and latency in communication equal to 10 ms were imposed in both directions. Finally, the controller tries to reclose the faulty feeder with a delay of 50 ms after the sources are reconnected. In the simulation included in this section, at time $t = 0.2$ s, a fault occurs at Load 2, and it is extinguished at time $t = 0.3$ s. Looking at the voltage graph shown in Figure 11, it is possible to observe an immediate voltage drop when the fault occurs. In the first milliseconds, this voltage drop is limited by the current provided by all the converters, as shown in Figure 12, and remains quite contained. When the currents of the converters of Battery 1 and Inverter 1 reach the current threshold of 375 A, the HCBs of both components are open. This happens after the fault recognition by the centralized controller but before it can signal it to the breakers. This is due to the communication latency of 10 ms. After the fault identification, the tripping of the HCBs of Inverter 1 and Battery 1 causes a further rapid decrease in the voltage,

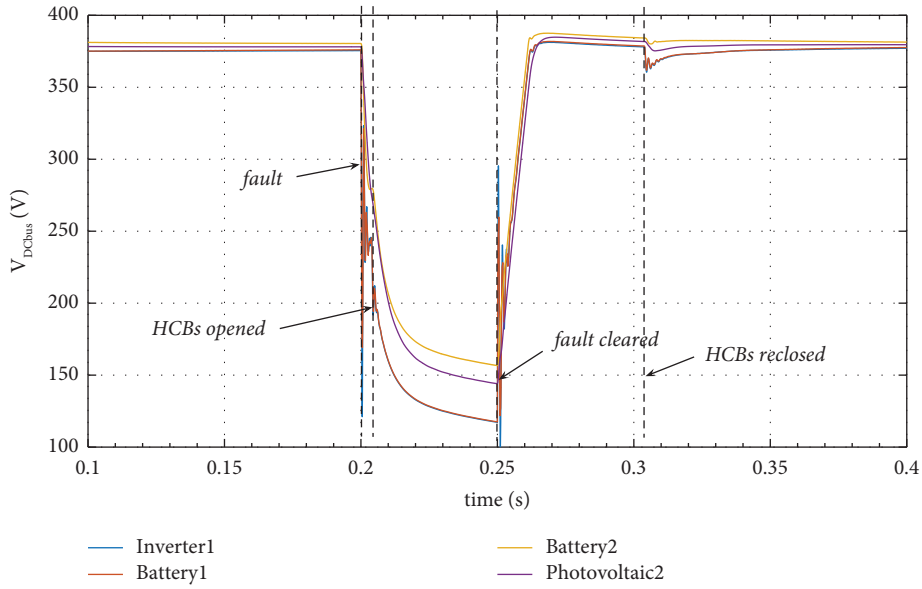

Figure 7: Voltage trend during short circuit with protection device.

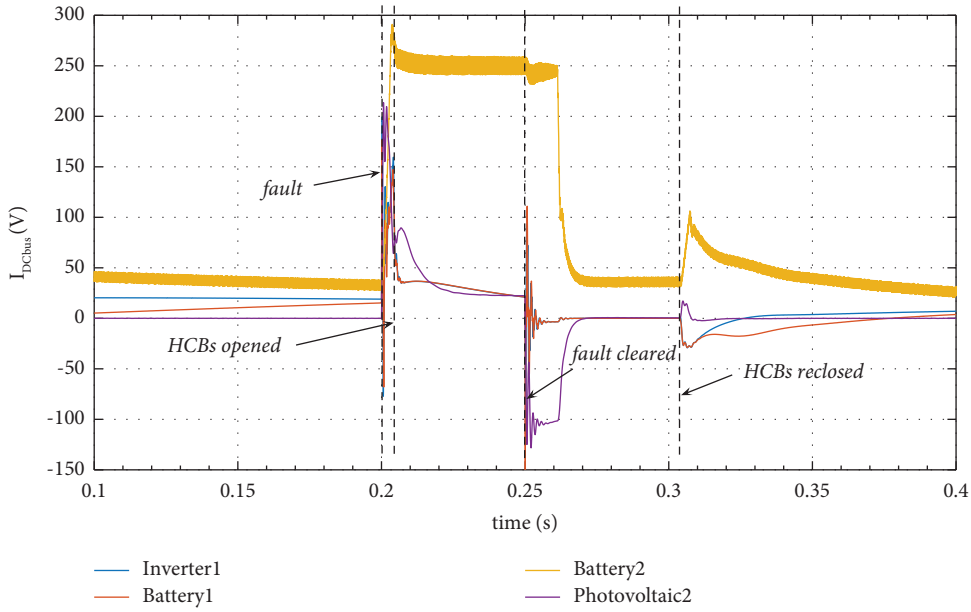

Figure 8: Current trend during short circuit with protection device.

which is sustained only by Battery 2 and the photovoltaic panels.

After identifying the faulty feeder, the controller reaches state 1 and sends a limitation command to the converters of Battery 2 and Photovoltaic 2. When both converters have limited their currents, the voltage drops because the grid is no longer supplied. After receiving the shut-down communication from the limited sources, the controller exits this state and enters state 2. As soon as the controller enters this state, it sends the trip signal to the breaker of the faulty feeder, where the current has already fallen below the threshold of 50 A and waits for an answer from it. After the recognition of this new state for the breaker, the controller sends a reset signal to the converters of the sources, which will be reconnected after a delay of 10 ms. The DC microgrid is thus re-energized, reaching the initial voltage condition. After a delay of 50 ms, the faulty feeder will be reconnected. In this situation, if the fault is not cleared, the previously described process is replicated until the maximum number of tolerated reclosures is reached. However, the controller returns to state 0 and waits for the possible recognition of another short-circuit condition.

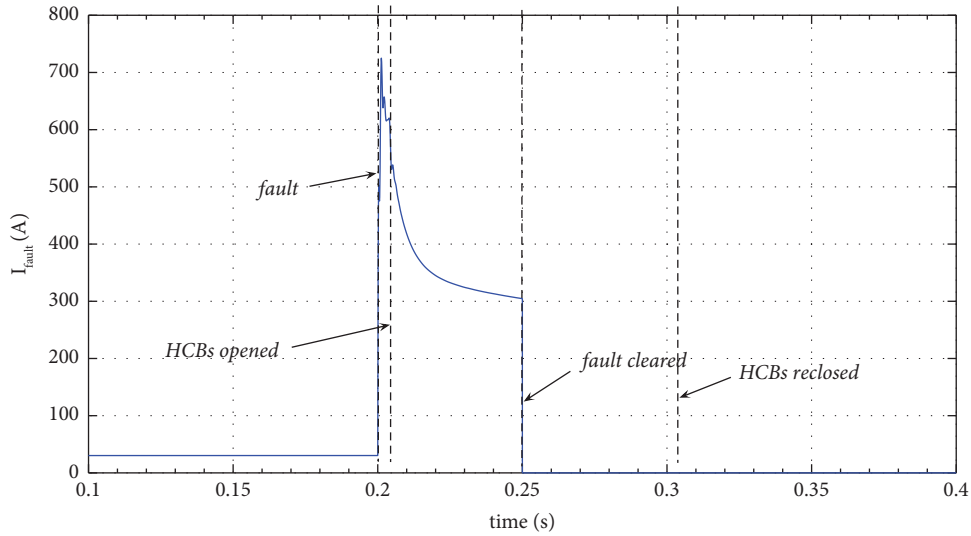

Figure 9: Current trend of load's feeder during short circuit.

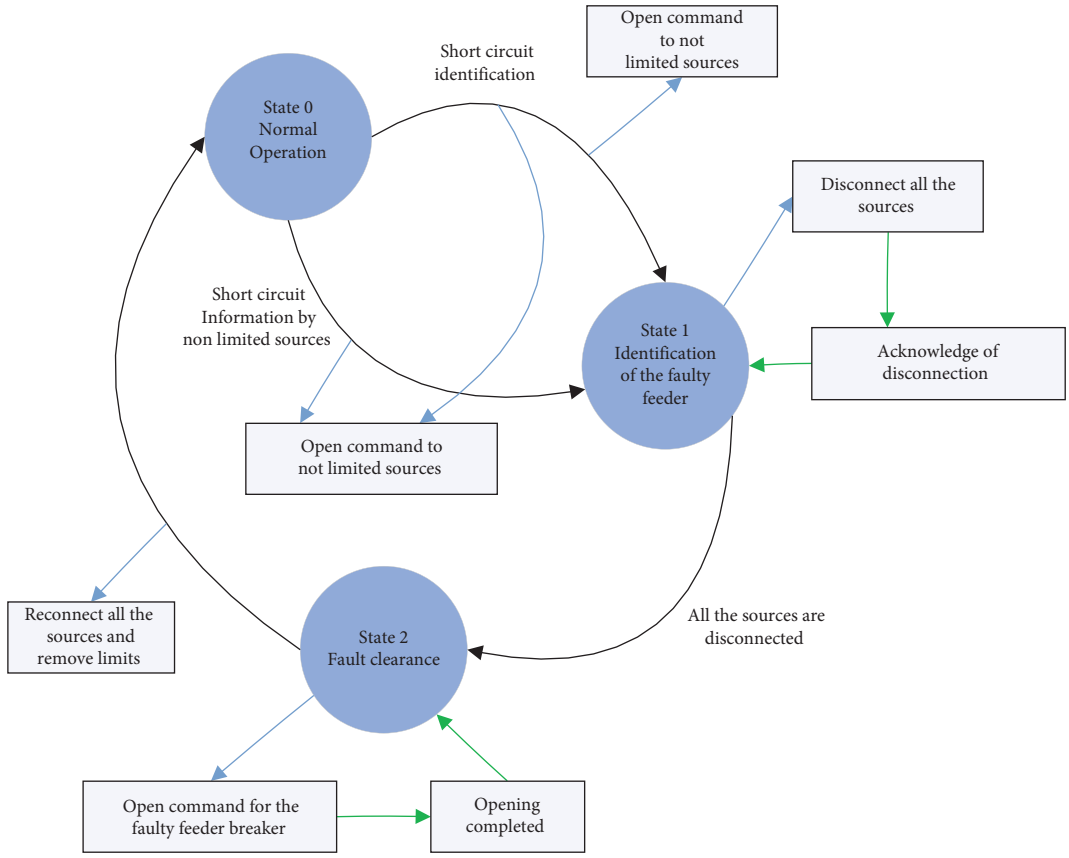

Figure 10: Centralized protection scheme.

4.2. Proposed Decentralized Protection Scheme. As previously explained, it is necessary to study a decentralized control scheme because it may not be possible or convenient to build the infrastructure required by a centralized controller. Furthermore, in the event of a failure of the communication system and therefore the impossibility of applying centralized control, each unit must still be able to intervene to ensure protection. It is also possible to design hybrid structures in which some sources are connected to the central controller and others work autonomously. This could be useful if some protection devices are distant and difficult to connect, and it allows a simple connection of new lines or new sources to the grid. In fact, in the case of a centralized structure, it is necessary to realize a wired

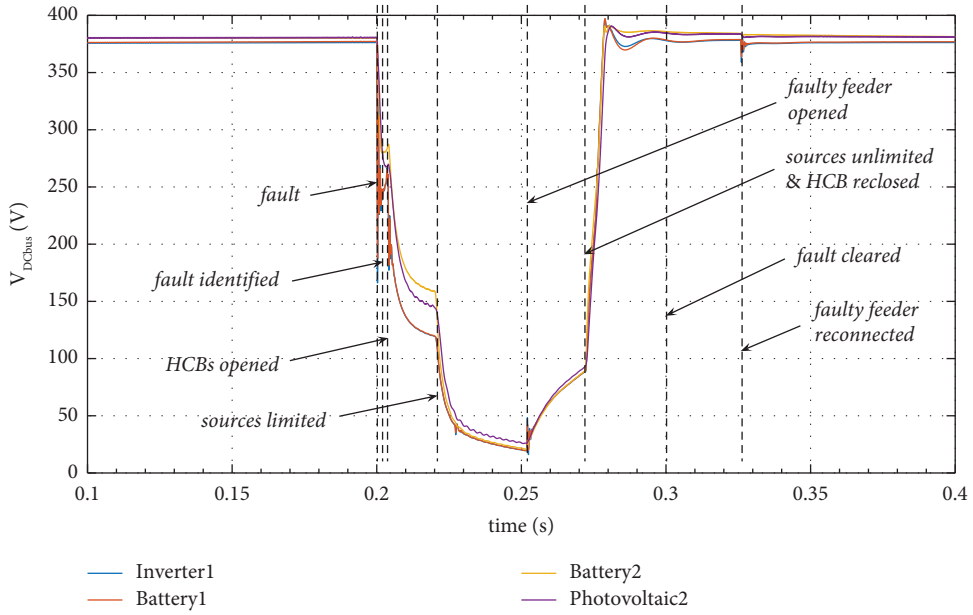

Figure 11: Voltage trend during short circuit with the centralized protection scheme.

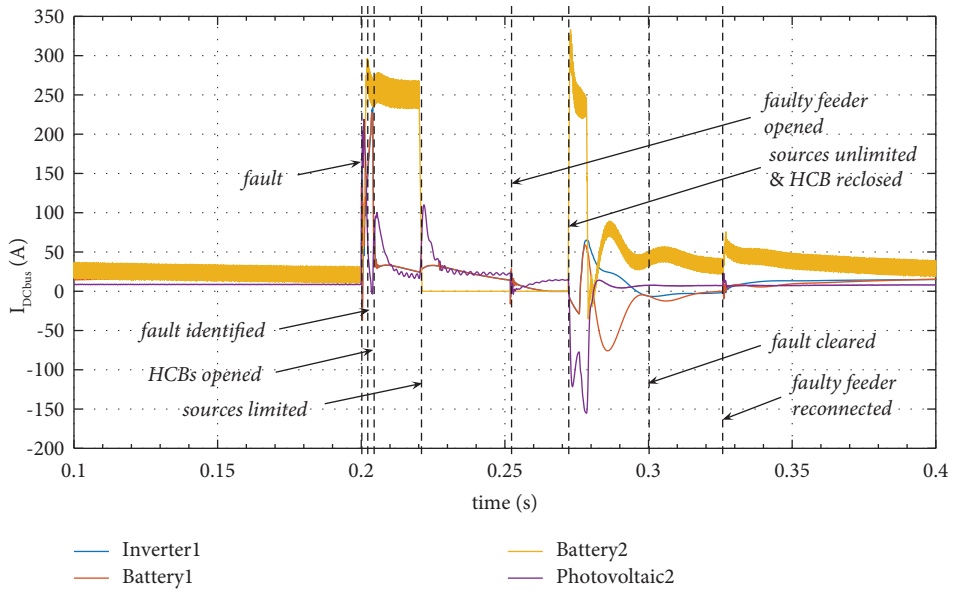

Figure 12: Current trend during short circuit with the centralized protection scheme.

communication system and reprogram the controller for each new source or line. Although the centralized controller can be programmed with vector logic precisely to reduce this problem, this may be costly, and at least temporarily, it might be useful to have a hybrid configuration. This paper does not analyse the hybrid structure, but it deals with the operation of a fully decentralized system that guarantees a backup for the controller-based system in the case of malfunctions.

The proposed coordination of protections, not only based on the time scale, is defined to ensure that the line breaker is opened if and only if its current is lower than the maximum for which the line switch was sized. The control of the sources is the same as the centralized strategy. Therefore, when a short circuit occurs on a line, the intrinsically nonlimited sources disconnect. If the intrinsically limited sources are limited or disconnected, the current in the faulty line (as in the others) is reduced and tends to zero. As soon as the current in the faulty line drops below the maximum manageable current, the breaker must open. This means that to ensure the intervention at a low current of the MCB, the fault is detected if the current exceeds the maximum current of the breaker, even for a single moment, and then, as soon as the current drops below the maximum, the switch is enabled

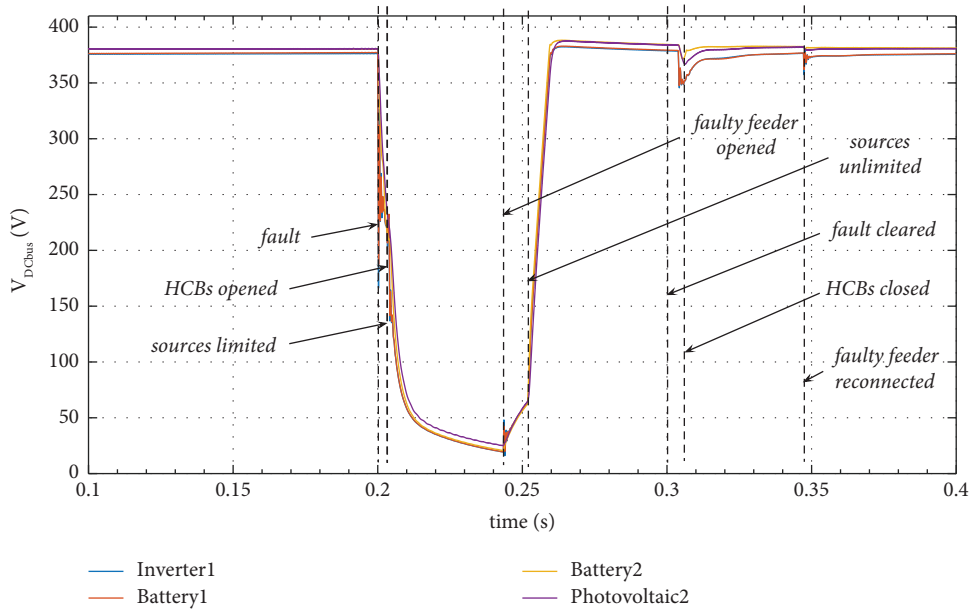

Figure 13: Trend of the voltage during a short circuit with the decentralized protection scheme.

to intervene. In this way, the opening of the faulty line takes place as quickly as possible. Thus, this decentralized control can be faster than the centralized one if the central controller's communication latency is significant.

Once the faulty line is opened, the sources can be reconnected. However, in this case, no information about the successful opening is available. It is then necessary to schedule an automatic reclosure after a fixed time. This time must allow the line switch to intervene. Because the operation only occurs when the current on the faulty line has become low, the time it takes depends on the fault location and on the line capabilities to discharge on the fault. Consequently, this time can vary by case and could be sized differently for different networks. In the test grid, it was observed from the simulations shown for the centralized controller that the time the current took to drop below the threshold was on the order of a few tens of milliseconds. Therefore, the decision was made to insert an automatic reclosure of the nonlimited sources after 100 ms.

The decentralized protection scheme was tested using the same numerical simulation used for the centralized one, considering a current threshold of 375 A and a voltage threshold of 300 V for the HCBs. The voltage threshold of the limited sources was set at the same value, while the current threshold was equal to the nominal current of the devices. Looking at the voltage graph shown in Figure 13, it is possible to observe an immediate voltage drop when the fault occurs. In this case, in contrast to the centralized protection scheme, Battery 2 does not supply the DC grid. Indeed, this source is instantaneously limited, and its current reaches zero, as shown in Figure 14. However, the dc grid voltage is supplied by the photovoltaic panel, which is working at its' short-circuit current, and by the capacitor of the HCBs. When the current in the faulty feeder falls below the threshold of 50 A, its breaker opens. Then, 50 ms after the fault recognition, the limitation of Battery 2 is removed, and the DC grid voltage is restored to 380 A. In the same way, 100 ms after the fault recognition, also Battery 1 and Inverter 1 are reconnected. Finally, the Load 2 breaker tries a reclosure after 100 ms, when the DC grid has already reached a stable operation.

4.3. Comparison of Control Strategies. To compare the behaviour and verify the feasibility of the two protection schemes, some tests were performed considering different fault locations: Load 2, Inverter 1, Battery 1, and Battery 2. The tests were performed as explained in the previous sections considering a fault resistance of 10 mΩ. From the analysis of the results, both protection schemes could guarantee the protection of the DC grid and the isolation of the faulty feeder. As shown in Figure 15, the fault location influences the fault current, which is the maximum in the case of a fault near the nonlimited sources. This faulty current is indeed provided by the output capacitor of the HCB, which discharges directly on the fault. Furthermore, the voltage reaches a minimum value in the case of a fault near Battery 2. In this situation, Battery 2 is indeed disconnected by its circuit breaker, and the DC grid is not supplied, until the reconnection of the nonlimited sources. Moreover, in this situation, the voltage dip duration is the highest, and in the case of the decentralized control, it reaches a value of about 100 ms. This time is equal to the automatic reclosure delay of the nonlimited sources.

It is worth noting that the two protection schemes also have nearly the same performances considering the current provided by all the sources during the fault, as shown in Figure 16. It is therefore possible to use both protection schemes. In general, the centralized controller allows better coordination of the different protections

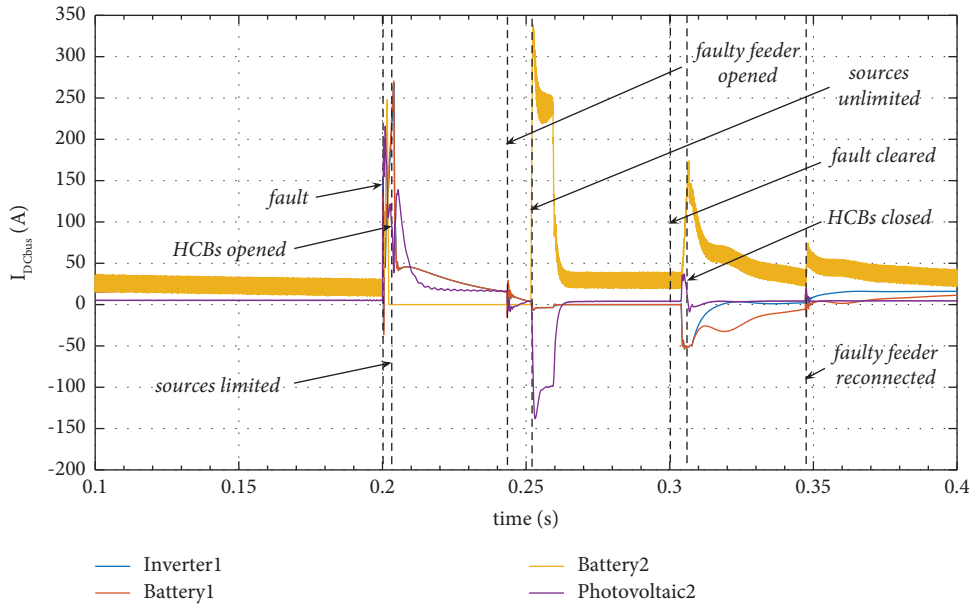

Figure 14: Current trend during short circuit with the decentralized protection scheme.

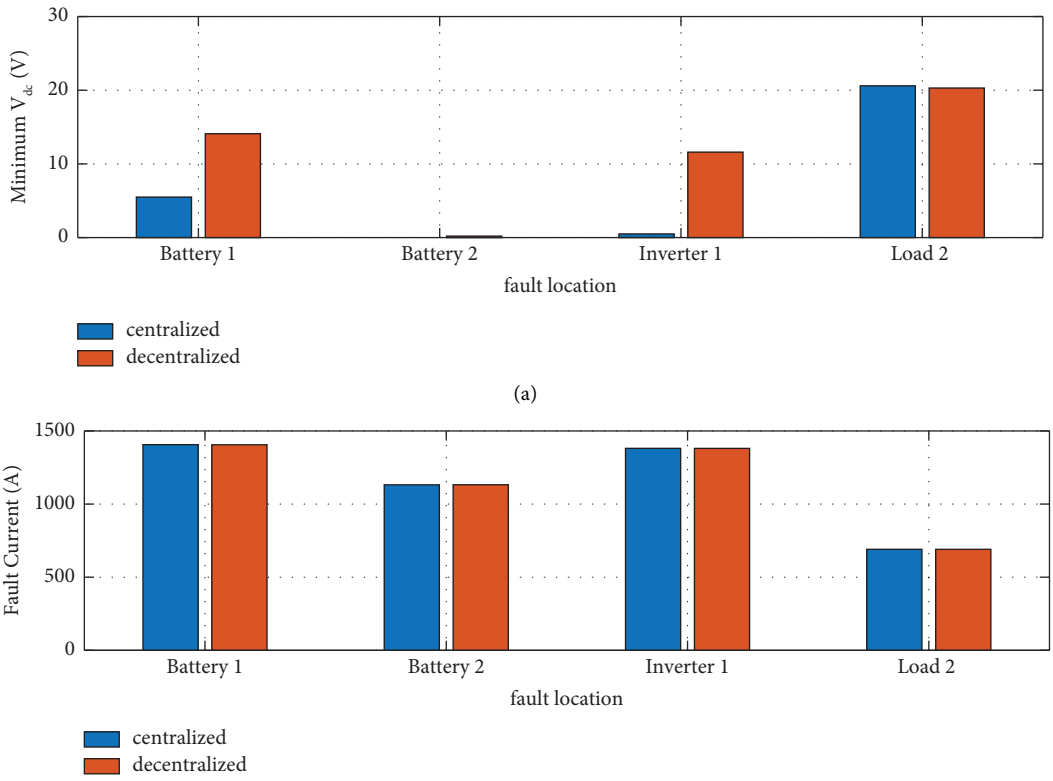

Figure 15: Continued.

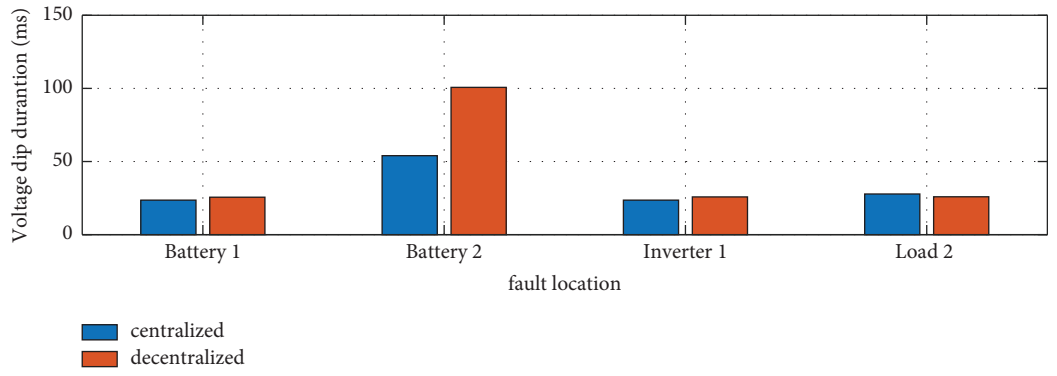

(c)

FIGURE 15: Comparison between centralized (blue) and decentralized (orange) protection schemes: (a) minimum voltage during a fault, (b) maximum fault current, and (c) voltage dip duration.

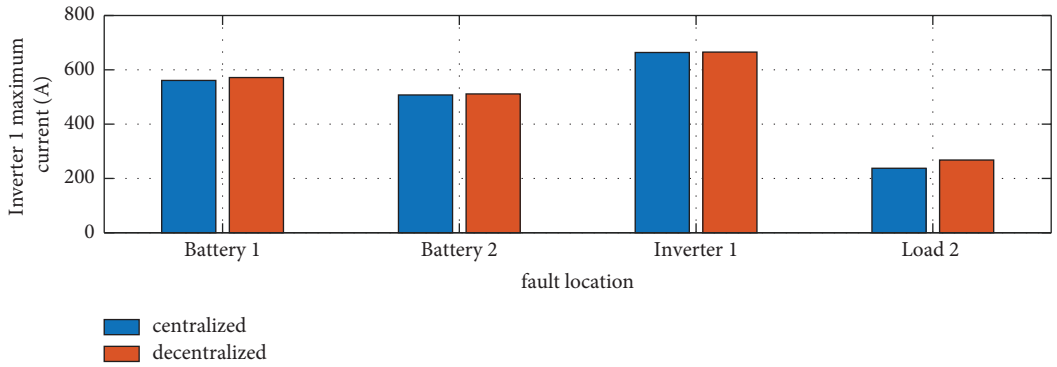

(a)

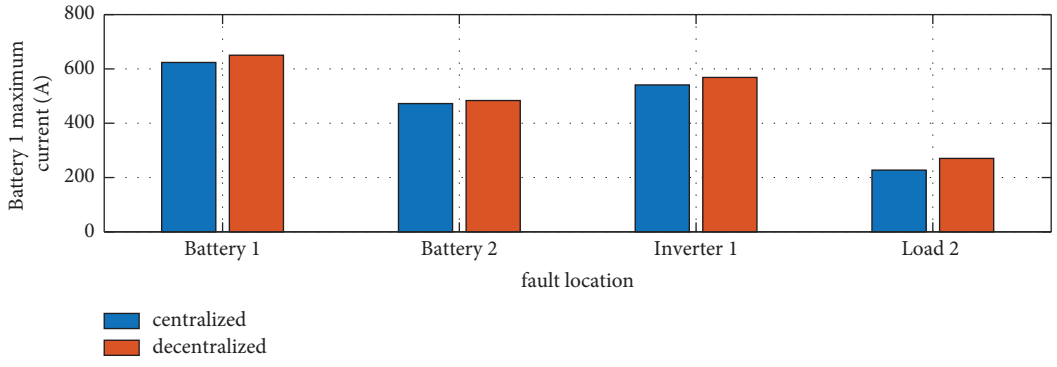

(b)

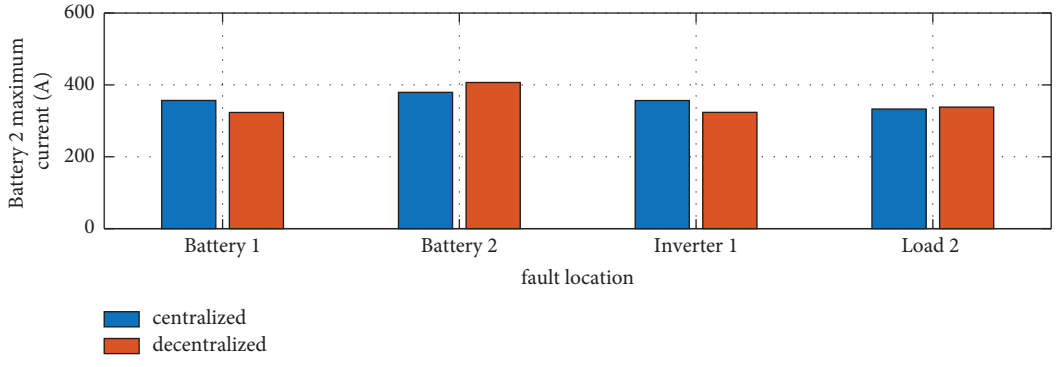

(c)

FIGURE 16: Comparison between centralized (blue) and decentralized (orange) protection schemes: (a) Inverter 1 current, (b) Battery 1 current, and (c) Battery 2 current.

thanks to a complete knowledge of the grid. However, this solution increases the overall installation cost, and in the case of a communication failure, the system is not able to intervene to ensure protection. For this reason, the decentralized scheme can be used as a backup system for a controller-based system in the case of malfunctions.

5. Conclusion

In the paper, the protection of a DC microgrid in the presence of a pole-to-pole fault is addressed by considering the combination of HCBs, capable of tripping the circuit during a fault condition, and MCBs. The use of these breakers reduces energy losses, but MCBs introduce further issues due to slow transition times and their inability to open in the presence of high currents without lifetime degradation. A new protection scheme completely decentralized is proposed in this paper. The proposed protection scheme is compared with the centralized scheme of [26], that resorting to all the DC grid information determines the fault location and allows the isolation of the faulty feeder. On the contrary, the proposed protection scheme does not need any information exchange among the converters and the protection devices and can be used as a backup system to improve the reliability of the system.

The analysis was performed through a test DC microgrid connected to the AC main grid and composed of several generators, loads, and storage systems interfaced through different converters. The simulations carried out through this benchmark DC microgrid allowed the identification of the requirements in terms of protection devices for each typology of the converter in case of pole-to-pole fault. It was verified that protection devices capable of interrupting a short-circuit current, such as the HCB considered in the paper, must be used only to protect nonlimited sources and connected to the grid using VSCs or boost converters. Conversely, the feeders and the limited sources can be protected by resorting to mechanical circuit breakers and applying the protection scheme defined in the paper. Indeed, resorting to this scheme, it is possible to identify the faulty feeder and reduce the faulty current in some milliseconds before the trip of the MCBs. The proposed decentralized protection scheme overcomes the fast fault-clearing time and selectivity issues in the case of a pole-to-pole fault. This solution, as demonstrated by several simulations, permits the coordination of MCBs and HCBs and avoids the use of SSCBs, bringing advantages in terms of energy efficiency.

Data Availability

The DC microgrid benchmark data used to support the findings of this study are included in the tables of the article.

Conflicts of Interest

The authors declare that they have no conflicts of interest.

Acknowledgments

This research was funded by the Ministry of Ecological Transition under the contract agreement "Accordo di Programma Mission Innovation 2021–2024" –project "MISSION-Multivector Integrated Smart Systems and Intelligent microgrids for accelerating the energy transition."

References

[1] T. Castillo-Calzadilla, M. A. Cuesta, C. Olivares-Rodriguez, A. M. Macarulla, J. Legarda, and C. E. Borges, "Is it feasible a massive deployment of low voltage direct current microgrids renewable-based? A technical and social sight," *Renewable and Sustainable Energy Reviews*, vol. 161, 2022.

[2] P. Rodriguez and K. Rouzbehi, "Multi-terminal dc grids: challenges and prospects," *Journal of Modern Power Systems and Clean Energy*, vol. 5, no. 4, pp. 515–523, 2017.

[3] J. J. Justo, F. Mwasilu, J. Lee, and J. Jung, "AC-microgrids versus DC-microgrids with distributed energy resources: a review," *Renewable and Sustainable Energy Reviews*, vol. 24, pp. 387–405, 2013.

[4] L. Pellegrino, R. Lazzari, and F. Almasio, "Energetic and economical analysis for an LVDC residential district," in *Proceedings of the AEIT International Annual Conference*, pp. 1–6, Bari, Italy, October 2018.

[5] T. Dragicevic, J. C. Vasquez, J. M. Guerrero, and D. Skrlec, "Advanced LVDC Electrical Power Architectures and Microgrids: a step toward a new generation of power distribution networks," *IEEE Electrification Magazine*, vol. 2, no. 1, pp. 54–65, 2014.

[6] N. R. Watson and J. D. Watson, "An overview of HVDC technology," *Energies*, vol. 13, no. 17, p. 4342, 2020.

[7] R. Ryndzionek and Ł. Sienkiewicz, "Evolution of the HVDC link connecting offshore wind farms to onshore power systems," *Energies*, vol. 13, no. 8, p. 1914, 2020.

[8] E. Pierri, O. Binder, N. G. Hemdan, M. Kurrat, and M. Kurrat, "Challenges and opportunities for a European HVDC grid," *Renewable and Sustainable Energy Reviews*, vol. 70, pp. 427–456, 2017.

[9] M. Fotopoulou, D. Rakopoulos, D. Trigkas, F. Stergiopoulos, O. Blanas, and S. Voutetakis, "State of the art of low and medium voltage direct current (DC) microgrids," *Energies*, vol. 14, no. 18, p. 5595, 2021.

[10] K. Jithin, P. P. Haridev, N. Mayadevi, R. H. Kumar, and V. P. Mini, "A review on challenges in DC microgrid planning and implementation," *Journal of Modern Power Systems and Clean Energy*, vol. 21, 2022.

[11] M. Cucuzzella, R. Lazzari, S. Trip, S. Rosti, C. Sandroni, and A. Ferrara, "Sliding mode voltage control of boost converters in DC microgrids," *Control Engineering Practice*, vol. 73, pp. 161–170, 2018.

[12] W. He, C. A. Soriano-Rangel, R. Ortega, A. Astolfi, F. Mancilla-David, and S. Li, "Energy shaping control for buck-boost converters with unknown constant power load," *Control Engineering Practice*, vol. 74, pp. 33–43, 2018.

[13] S. Ansari, J. Zhang, and R. E. Singh, "A review of stabilization methods for DCMG with CPL, the role of bandwidth limits and droop control," *Protection and Control of Modern Power Systems*, vol. 7, no. 1, 2022.

[14] S. Singh, A. R. Gautam, and D. Fulwani, "Constant power loads and their effects in DC distributed power systems: a review," *Renewable and Sustainable Energy Reviews*, vol. 72, pp. 407–421, 2017.

[15] M. Cupelli, L. Zhu, and A. Monti, "Why ideal constant power loads are not the worst-case condition from a control standpoint," *IEEE Transactions on Smart Grid*, vol. 6, no. 6, pp. 2596–2606, 2015.

[16] R. M. Cuzner and G. Venkataramanan, "The status of DC micro-grid protection," in *Proceedings of the Industry Applications Society Annual Meeting*, pp. 1–8, Edmonton, AB, Canada, October 2008.

[17] A. A. S. Emhemed and G. M. Burt, "An advanced protection scheme for enabling an LVDC last mile distribution network," *IEEE Transactions on Smart Grid*, vol. 5, no. 5, pp. 2602–2609, 2014.

[18] D. M. Bui, S. L. Chen, and C. H. Wu, "Review on protection coordination strategies and development of an effective protection coordination system for DC microgrid," in *Proceedings of the IEEE PES Asia-Pacific Power and Energy Engineering Conference (APPEEC)*, pp. 1–10, Hong Kong, China, December 2014.

[19] C. Peng and A. Q. Huang, "A protection scheme against DC faults VSC based DC systems with bus capacitors," in *Proceedings of the IEEE Applied Power Electronics Conference and Exposition (APEC)*, pp. 3423–3428, Fort Worth, TX, USA, March 2014.

[20] M. E. Baran and N. R. Mahajan, "Overcurrent protection on voltage-source-converter based multiterminal DC distribution systems," *IEEE Transactions on Power Delivery*, vol. 22, no. 1, pp. 406–412, 2007.

[21] M. Farhadi and O. A. Mohammed, "Protection of multiterminal and distributed DC systems: design challenges and techniques," *Electric Power Systems Research*, vol. 143, pp. 715–727, 2017.

[22] G. Patil and M. F. A. R. Satarkar, "Autonomous protection of low voltage DC microgrid," in *Proceedings of the International Conference on Power, Automation and Communication (INPAC)*, pp. 23–26, Amravati, India, October 2014.

[23] S. Beheshtaein, R. M. Cuzner, M. Forouzesh, M. Savaghebi, and J. M. Guerrero, "DC microgrid protection: a comprehensive review," *IEEE Journal of Emerging and Selected Topics in Power Electronics*, vol. 4, 2016.

[24] J. C. Hernández, F. S. Sutil, and P. G. Vidal, "Protection of a multiterminal DC compact node feeding electric vehicles on electric railway systems, secondary distribution networks, and PV systems," *Turkish Journal of Electrical Engineering and Computer Sciences*, vol. 24, no. 4, pp. 3123–3143, 2016.

[25] R. Lazzari and L. Piegari, "Design and implementation of LVDC hybrid circuit breaker," *IEEE Transactions on Power Electronics*, vol. 34, no. 8, pp. 7369–7380, 2019.

[26] R. Lazzari and L. Piegari, "Analysis and design of the protection scheme for an LVDC microgrid," in *Proceedings of the International Conference on Clean Electrical Power (ICCEP)*, pp. 639–644, Otranto, Italy, October 2019.

[27] S.-M. Xue and C. Liu, "Line-to-Line fault analysis and location in a VSC-based low-voltage DC distribution network," *Energies*, vol. 11, no. 3, p. 536, 2018.

[28] R. Lazzari, L. Piegari, S. Grillo et al., "Selectivity and security of DC microgrid under line-to-ground fault," *Electric Power Systems Research*, vol. 165, pp. 238–249, 2018.

[29] L. Zhang, N. Tai, W. Huang, J. Liu, and Y. Wang, "A review on protection of DC microgrids," *Journal of Modern Power Systems and Clean Energy*, vol. 6, pp. 1113–1127, 2018.

[30] J. Yang, J. E. Fletcher, and J. O'Reilly, "Short-circuit and ground fault analyses and location in VSC-based DC network cables," *IEEE Transactions on Industrial Electronics*, vol. 59, no. 10, pp. 3827–3837, 2012.

[31] W. Rieder, "Circuit breakers physical and engineering problems I-fundamentals," *IEEE Spectrum*, vol. 7, no. 7, pp. 35–43, 1970.

[32] A. Shukla and G. D. Demetriades, "A survey on hybrid circuit-breaker topologies," *IEEE Transactions on Power Delivery*, vol. 30, no. 2, pp. 627–641, 2015.

[33] R. Rodrigues, Y. Du, A. Antoniazzi, and P. Cairoli, "A review of solid-state circuit breakers," *IEEE Transactions on Power Electronics*, vol. 36, no. 1, pp. 364–377, 2021.

[34] A. A. S. Emhemed, K. Fong, S. Fletcher, and G. M. Burt, "Validation of fast and selective protection scheme for an LVDC distribution network," *IEEE Transactions on Power Delivery*, vol. 32, no. 3, pp. 1432–1440, 2017.

[35] G. Madingou, M. Zarghami, and M. Vaziri, "Fault detection and isolation in a DC microgrid using a central processing unit," in *Proceedings of the 2015 IEEE Power and Energy Society Innovative Smart Grid Technologies Conference (ISGT)*, pp. 1–5, Washington, DC, USA, February 2015.

[36] N. Bayati, A. Hajizadeh, and M. Soltani, "Protection in DC microgrids: a comparative review," *IET Smart Grid*, vol. 1, no. 3, pp. 66–75, 2018.

[37] M. Monadi, M. Amin, J. Ignacio Candela, A. Luna, and P. Rodriguez, "Protection of AC and DC distribution systems Embedding distributed energy resources: a comparative review and analysis," *Renewable and Sustainable Energy Reviews*, vol. 51, pp. 1578–1593, 2015.

[38] C. Srivastava and M. Tripathy, "DC microgrid protection issues and schemes: a critical review," *Renewable and Sustainable Energy Reviews*, vol. 151, p. 111546, 2021.

[39] M. Muniappan, "A comprehensive review of DC fault protection methods in HVDC transmission systems," *Protection and Control of Modern Power Systems*, vol. 6, p. 1, 2021.

[40] E. Christopher, M. Sumner, D. W. P. Thomas, X. Wang, and F. de Wildt, "fault location in a zonal DC marine power system using active impedance estimation," *IEEE Transactions on Industry Applications*, vol. 49, no. 2, pp. 860–865, 2013.

[41] S. Papathanassiou, N. Hatziargyriou, and K. Strunz, "A benchmark for low voltage microgrid network," in *Proceedings of the CIGRE Symposium Power Systems with Dispersed Generation*, Athens, Greece, June 2005.

[42] L. Piegari and R. Rizzo, "Adaptive perturb and observe algorithm for photovoltaic maximum power point tracking," *IET Renewable Power Generation*, vol. 4, no. 4, pp. 317–328, 2010.